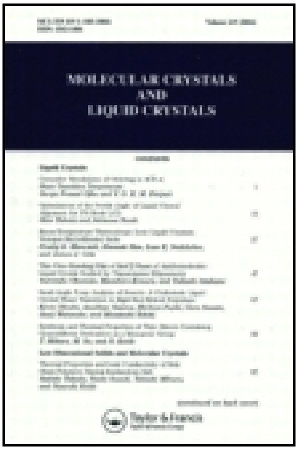

Molecular Crystals and Liquid Crystals
Publication details, including instructions for authors and subscription information:
http://www.tandfonline.com/loi/gmcl20

Synthesis and Mesomorphic Properties of Low Molar Mass Phosphorus Derivatives

N. Tokushige [a] , T. Mihara [a] & N. Koide [a]
[a] Department of Chemistry, Faculty of Science, Science University of Tokyo, 1-3 Kagurazaka, Shinjuku-ku, Tokyo, 162-8601, Japan

Version of record first published: 18 Oct 2010

To cite this article: N. Tokushige, T. Mihara & N. Koide (2004): Synthesis and Mesomorphic Properties of Low Molar Mass Phosphorus Derivatives, Molecular Crystals and Liquid Crystals, 414:1, 27-38

To link to this article: http://dx.doi.org/10.1080/15421400490427421

Mol. Cryst. Liq. Cryst., Vol. 414, pp. 27–38, 2004

ISSN: 1542-1406 print/1563-5287 online
DOI: 10.1080/15421400490427421

SYNTHESIS AND MESOMORPHIC PROPERTIES OF LOW MOLAR MASS PHOSPHORUS DERIVATIVES

N. Tokushige, T. Mihara, and N. Koide
Department of Chemistry, Faculty of Science,
Science University of Tokyo, 1-3 Kagurazaka, Shinjuku-ku,
Tokyo 162-8601, Japan

New liquid crystalline phosphorus derivatives were synthesized as a core model compound and/or a model compound of the component for semiflexible liquid crystalline polymers. Alkoxy, oligo ethylene oxide, or chiral moieties were introduced into the terminal group of rigid moiety in order to investigate the effect of the terminal group on the thermal properties of the phosphorus derivatives. A nematic phase appears for the phosphorus derivative with alkoxy moieties or oligo ethylene oxide chain, while a mesophase is observed for the phosphorus derivative with a chiral moiety. Some phosphorus derivatives were thermally stable until more than 300°C.

Keywords: liquid crystal; phosphorus derivative

INTRODUCTION

Generally, phosphorus compounds, organic bromine compounds, and inorganic compounds are used as a flame-retardant additive. At the present time, it is well known that phosphorus compounds are generally used as the most effective flame retardant additive for polymers. The flame retardant additives are used in relatively high concentration to enhance thermal stability of polymers. As a result, the use of the flame retardant additives can lead to undesirable changes in physical and mechanical properties of the polymers.

On the other hand, with regard to polymers without flame-retardant groups, the liquid crystalline (LC) polyesters themselves have good flame-retardant properties and exhaust carbon dioxide in the combustion process; however, the flame-retardant properties of the LC polyesters are not adequate for processability conditions such as high temperature and pressure.

Address correspondence to N. Koide, e-mail: nkoide@ch.kagu.sut.ac.jp

Copolyesters (polyethylene naphthalate and polybutylene naphthalate) containing phosphorus compounds were prepared by copolymerization of naphthalene derivative and phosphorus compound [1]. Moreover, various polyphosphates were reported by Kishore et al. [2–5].

Senthil et al. reported synthesis and characterization of metallomesogenic semiflexible liquid crystalline polymers (LCPs) containing a nonmesogenic phosphorus derivative [6,7]. The effect of the phosphorus derivative in the spacer and metallomesogen on the thermal properties were examined.

The flame-retardant properties of LCP can be greatly enhanced by introducing the phosphorus derivative to the LCP. Generally, it is necessary to attach mesomorphic properties to phosphorus derivatives as a component for semiflexible LCPs to enhance the liquid crystallinity of semiflexible LCPs or to avoid reduction of the liquid crystallinity of semiflexible LCPs. However, the phosphorus derivatives with mesomorphic properties are little investigated. In this study, we synthesized novel low molar mass phosphorus derivatives as a core model compound and/or a model compound of the component for semiflexible LCPs, as shown in Figure 1, and investigated the thermal properties by polarized optical microscope, differential scanning calorimetry (DSC) measurements, and thermogravimetric analysis (TGA). Furthermore, the structure of the mesophase of the phosphorus derivatives was examined by X-ray measurements.

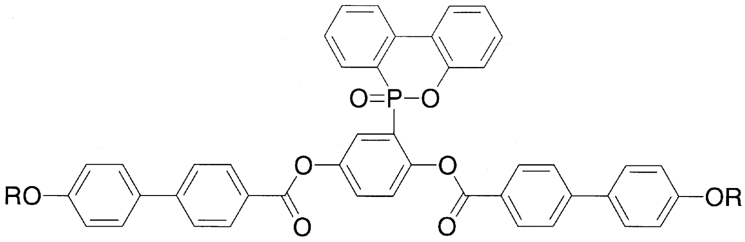

R = $CH_3(CH_2)_5$	6O-PD
R = $CH_3(CH_2)_7$	8O-PD
R= $CH_3CH_2C^*H(CH_3)CH_2$	2MB-PD
R= $CH_3(OC_2H_4)_2$	2EO-PD

FIGURE 1 Chemical structure of phosphorus derivatives.

EXPERIMENTAL

Materials

The phosphorus derivatives were prepared according to Schemes 1 and 2. Typical procedures are described below.

4-(4-Hydroxyphenyl)benzoic acid methyl ester (1)

4-(4-Hydroxyphenyl)benzoic acid (5.0 g, 23.3 mmol) was dissolved in methanol (150 ml). Sulfuric acid (5.0 ml) was added dropwise to the methanol solution, and then the reaction mixture was refluxed for 6 h. After methanol was evaporated to dryness under reduced pressure, the residue was washed with water until a neutral aqueous solution was obtained. The white solid was obtained in a 97.0% yield (5.2 g).

IR (nujol) $\nu\,\mathrm{cm}^{-1}$: 3400 (OH, phenol), 1737 (C=O, ester), and 1605 and 1508 (aromatic group).

4-(4-Octyloxyphenyl)benzoic Acid (3)

The compound **1** (5.0 g, 21.9 mmol) was dissolved in 2-butanone (150 ml), and then potassium carbonate (9.0 g, 65.7 mmol) was added to the 2-butanone solution. The mixture was refluxed and then 1-bromooctane (12.6 g, 65.7 mmol) was added dropwise to the mixture. The reaction mixture was refluxed for 6 h. The filtrate was evaporated to dryness under reduced pressure and the ethanol (100 ml) was added to the residue. Potassium hydroxide (3.7 g, 65.7 mmol) aqueous solution (30 ml) was

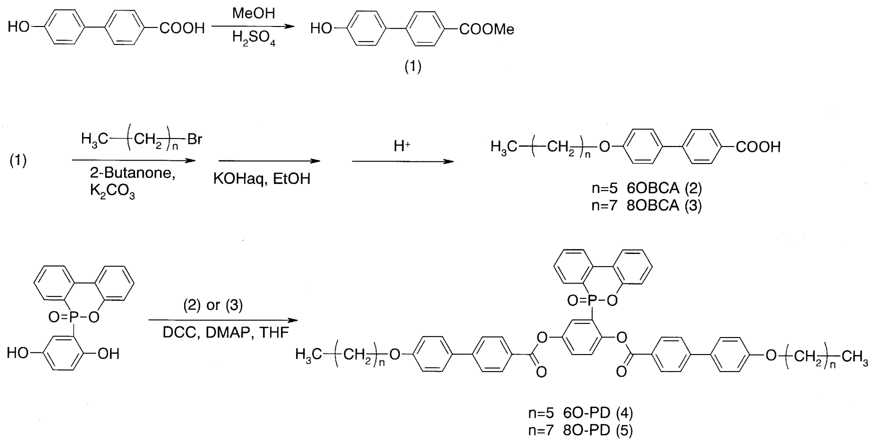

SCHEME 1 Synthesis of phosphorus derivatives (6O-PD and 8O-PD).

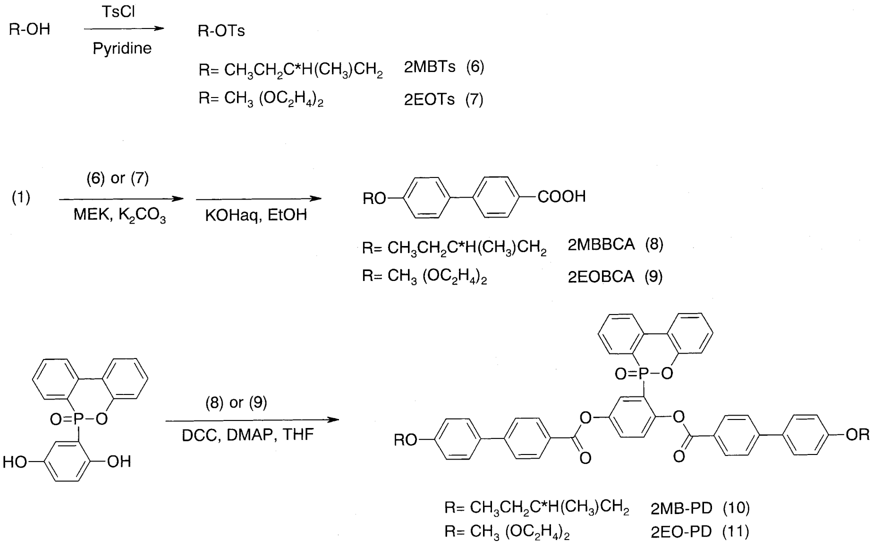

SCHEME 2 Synthesis of phosphorus derivatives (2MB-PD and 2EO-PD).

added to the ethanol solution and then the reaction mixture was refluxed for 30 min. Ethanol was evaporated and then HCl aqueous solution was added to the residue. The mixture was refluxed for 3 h. The precipitate obtained was washed with water. The solid was dried in vacuo and then washed with hexane. The product was obtained in a 74% yield (5.3 g). The product was used without further purification.

IR (nujol) $\nu\,\mathrm{cm}^{-1}$: 2723, 2678 (OH, carboxylic acid), 1685 (C=O, carboxylic acid), 1604 and 1504 (aromatic group), and 1252 ($Ar{-}O{-}CH_2$, ether). ^{1}H-NMR (DMSO) δppm: 0.9(t, 3H, CH_3), 1.2–1.8(m, 12H, CH_2), 4.0(t, 2H, $O{-}CH_2$), 7.0(d, 2H, Ar–H), 7.6–7.8(q, 4H, Ar–H), 8.0(d, 2H, Ar–H).

(2-Methoxyethoxy)ethyl Tosylate (7: 2EOTs)

Diethylene glycol monomethyl ether (20 g, 121 mmol) was dissolved in pyridine (200 ml). p-Toluenesulfonyl chloride (27 g, 141 mmol) was added to the pyridine solution in ice bath. The reaction mixture was stirred for 6 h. A large quantity of water was added to the reaction mixture in ice bath and then stirred for 6 h. The aqueous mixture was extracted with chloroform, and the chloroform solution was dried over magnesium sulfate. The chloroform was evaporated. The residual liquid was obtained in a 90% yield (35.2 g). The liquid was used without further purification.

2-Methylbutyl tosylate (6)

The compound **6** (2MBTs) was prepared according to the synthetic procedure of compound **5** (2EOTs). The liquid was obtained in an 84% yield. $[\alpha]_D^{25} = +2.0°$ (C=3, $CHCl_3$).

4-[4-(2-methylbutoxy)phenyl] Benzoic Acid (8: 2MBBCA)

The compound **1** (4.0 g, 17.5 mmol) was dissolved in 2-butanone (150 ml), and then potassium carbonate (7.3 g, 52.5 mmol) was added to the 2-butanone solution. The 2-butanone solution was refluxed and then the compound **4** (8.5 g, 35.0 mmol) was added dropwise to the 2-butanone solution. The reaction mixture was refluxed for 12 h. The filtrate was evaporated to dryness under reduced pressure, and then ethano (100 ml) was added to the residue. Potassium hydroxide (9.0 g, 157 mmol) aqueous solution (30 ml) was added to the ethanol solution and then the reaction mixture was refluxed for 30 min. Ethanol was evaporated and the HCl aqueous solution was added to the residue. The mixture was refluxed for 3 h. The precipitate obtained was washed with water. The solid was dried in vacuo, and then washed with hexane. The product was obtained in a 48% yield (2.4 g). The product was used without further purification. ^{1}H-NMR (DMSO) δ ppm: 0.95–1.1(m, 6H, CH_3), 1.2(m, 1H, CH_2), 1.3(m, 1H, CH_2), 1.9(m, 1H, CH), 3.9(m, 2H, $O{-}CH_2$), 7.1(d, 2H, Ar–H), 7.7–7.8(q, 4H, Ar–H), 8.0(d, 2H, Ar–H).

4-{4-[2-(2-Methoxyethoxy)ethoxy]phenyl} Benzoic Acid (9: 2EOBCA)

The compound **9** (2EOBCA) was prepared according to the synthetic procedure of the compound **8**. ^{1}H-NMR ($CDCl_3$) δ ppm: 3.3(s, 3H, CH_3), 3.6(d, 2H, $O{-}CH_2$), 3.7(d, 2H, $O{-}CH_2$), 3.8(d, 2H, $O{-}CH_2$), 4.1(d, 2H, $O{-}CH_2$), 6.9(d, 2H, Ar–H), 7.5(d, 2H, Ar–H), 7.6(d, 2H, Ar–H), 8.1(d, 2H, Ar–H).

80-PD (5)

The compound **3** (1.8 g, 4.3 mmol) and 2-(6-oxide-6H-dibenz ⟨c,e⟩ ⟨1,2⟩ oxaphosphorin-6-yl]-1,4-benzenediol (0.7 g, 2.2 mmol) were dissolved in tetrahydrofuran (THF, 150 ml) under nitrogen atmosphere. 4-Dimethylaminopyridine (0.07 g, 0.55 mmol) was added to the THF solution, and then a THF solution (30 ml) of N,N′-dicyclohexylcarbodiimide (2.7 g, 13.2 mmol) was added dropwise to the THF solution in ice bath. The reaction mixture was stirred for 6 h. After filtration, THF was evaporated to dryness under reduced pressure. The residue was washed with water and methanol. The crude product was purified by recrystallization from mixed solvent of chloroform and methanol (chloroform/methanol = 3/1). The white solid was obtained in a 28% yield (0.5 g).

IR (nujol) $\nu\,\mathrm{cm}^{-1}$: 1726 (COO, ester group), 1604 and 1496 (aromatic group). ^{1}H-NMR ($CDCl_3$) δ ppm: 0.9(m, 6H, CH_3), 1.3–1.6(m, 4H, CH_2), 1.8(m, 4H, CH_2), 4.0(m, 4H, O$-$$CH_2$), 7.0–8.2(m, 27H, Ar$-$H).

60-PD, 2MB-PD, and 2EO-PD

60-PD, 2MB-PD, and 2EO-PD were prepared according to the synthetic procedure of 8O-PD.

2MB-PD was obtained in a 58% yield. IR (nujol) $\nu\,\mathrm{cm}^{-1}$: 1733 (COO, ester group), and 1604 and 1496 (aromatic group). ^{1}H-NMR ($CDCl_3$) δ ppm: 0.9–1.0(m, 12H, CH_3), 1.3(m, 2H, CH), 1.5(m, 2H, CH_2), 1.8(m, 2H, CH_2), 3.8(m, 4H, O$-$$CH_2$), 6.9–8.2(m, 27H, Ar$-$H).

$$[\alpha]_D^{25} = +0.05^\circ \text{ (C=3, } CHCl_3).$$

2EO-PD was obtained in a 27% yield. IR (nujol) $\nu\,\mathrm{cm}^{-1}$: 1731 (COO, ester group), and 1604 and 1496 (aromatic group). ^{1}H-NMR ($CDCl_3$) δ ppm: 3.3(d, 6H, CH_3), 3.5(q, 4H, O$-$$CH_2$), 3.7(q, 4H, O$-$$CH_2$), 3.8(q, 4H, O$-$$CH_2$), 4.1(q, 4H, O$-$$CH_2$), 7.0–8.2(m, 27H, Ar$-$H).

Characterization

^{1}H-NMR was carried out with a JEOL JNM-LA 400 spectrometer using $CDCl_3$ as the solvent. Infrared spectra were recorded on JEOL JIR 7000 spectrometer. Spectra were collected at 4 cm^{-1} resolution. DSC measurements were conducted with a Mettler DSC821^e. Entropy changes from mesophase to isotropic phase (ΔS_{MI}) of phosphorus derivatives were obtained by the equation, $\Delta S_{MI} = \Delta H_{MI}/T$. TGA was carried out using a Mettler TG50 system in air. Optical microscopy measurements were performed on a Nikon polarizing optical microscope, OPTIPHOTO-POL, equipped with a Mettler FP80 controller and a FP82 hot stage. X-ray diffraction patterns were recorded with a RIGAKU RINT2500 with Ni-filtered CuKα radiation. The sample in quartz capillary (diameter 1 mm) was held in a temperature-controlled cell (RIGAKU LC high temperature controller). Optical rotation was recorded with a HORIBA SEPA-300 optical rotatory dispersion spectrometer. The sample was prepared using chloroform as a solvent.

RESULTS AND DISCUSSION

Synthesis of the phosphorus derivatives is described in Schemes 1 and 2. Thermal properties of the phosphorus derivatives are summarized in Table 1. A schlieren texture or a thread texture is observed on both heating and cooling runs for 6O-PD, 8O-PD, and 2EO-PD, as shown in Figures 2(a), 2(b), and 2(d). The schlieren texture of 2EO-PD is preserved at room

TABLE 1 Thermal Properties of Phosphorus Derivatives

Phosphorus derivatives	Phase transition temperatures/°C	$\Delta S_{MI}/(\mathrm{Jmol}^{-1}\mathrm{K}^{-1})^a$	$T_d/°C^b$
60-PD	$\mathrm{Cr} \underset{164}{\overset{185}{\rightleftharpoons}} \mathrm{N} \underset{234}{\overset{235}{\rightleftharpoons}} \mathrm{I}$	5.2	365
80-PD	$\mathrm{Cr} \underset{162}{\overset{176}{\rightleftharpoons}} \mathrm{N} \underset{220}{\overset{220}{\rightleftharpoons}} \mathrm{I}$	3.1	295
2MB-PD	$\mathrm{Cr} \underset{\underset{178 \qquad 202}{\longleftarrow \mathrm{M} \longleftarrow}}{\xrightarrow{\qquad 207 \qquad}} \mathrm{I}$	3.9	358
2EO-PD	$\mathrm{g} \underset{39}{\overset{43}{\rightleftharpoons}} \mathrm{N} \underset{203}{\overset{204}{\rightleftharpoons}} \mathrm{I}$	4.2	322

g, glassy; Cr, crystal; N,nematic; M, mesophase; I, isotropic phase.

[a] Entropy change at clearing points by DSC measurements.

[b] Temperatures at which 10% weight loss was recorded by TGA measurements.

temperature. On the other hand, a focal conic texture appears for 2MB-PD on cooling run as shown in Figure 2(c). Generally, a focal conic texture appears in a smectic phase and a cholesteric phase with the

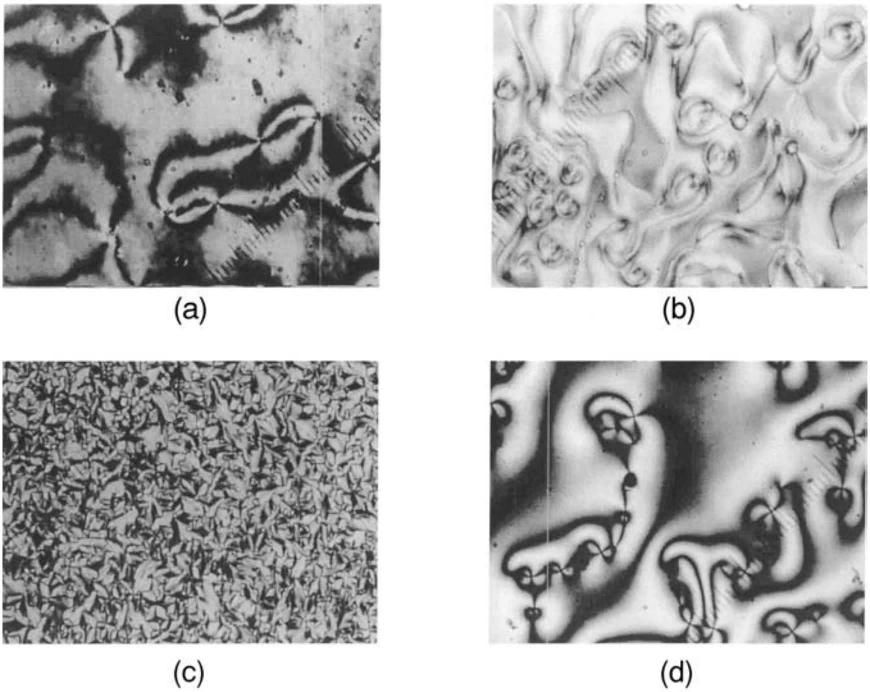

FIGURE 2 Optical textures of phosphorus derivatives; (a) 6O-PD at 230°C, (b) 8O-PD at 210°C, (c) 2MB-PD at 198°C, and (d) 2EO-PD at 200°C.

random alignment of helical axis. To assign the exact structure of the mesophases, the shear strain method offers a promising identification of a focal conic texture. A focal conic texture of a smectic phase appears again very soon after removing shear strain, while for a cholesteric phase, a planar texture instead of a focal conic texture is usually observed after removing shear strain. We imposed shear strain by shifting the glass substrate to confirm the structure of the mesophase for 2MB-PD. After removing shear strain for 2MB-PD, a planar texture of 2MB-PD forms and then a focal conic texture reappears.

Typical DSC curves of the phosphorus derivatives are shown in Figure 3. Two phase-transition peaks are observed on both heating and cooling runs for the phosphorus derivatives with terminal alkoxy chains (6O-PD and 8O-PD). Each peak is assigned to the melting and clearing points, respectively, based on the polarized microscope measurements. Mesomorphic temperature range of 6O-PD is wider than that of 8O-PD. With regard to 2MB-PD, which has chiral terminal moieties, a single peak appears on a heating run while two peaks are observed on a cooling run. This result indicates that 2MB-PD exhibits a monotropic mesophase. Glass transition temperature

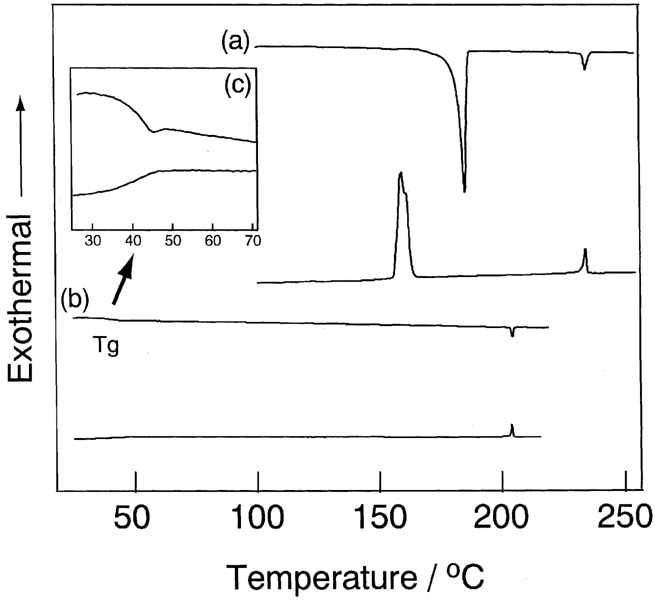

FIGURE 3 DSC curves of phosphorus derivatives; (a) 6O-PD, (b) 2EO-PD, and (c) expansion in the temperature range of 25–70°C for 2EO-PD.

and clearing point are observed in DSC curves of 2EO-PD. The structure of the mesophase for 2EO-PD is preserved at room temperature.

Only a broad peak in the wide angle region is observed in the X-ray pattern of 6O-PD at 200°C on cooling run as shown in Figure 4(a). The X-ray pattern and observation of a schlieren texture indicates that the structure of the mesophase for 6O-PD is a nematic phase. On the other hand, a peak in the small angle region and a broad peak in the wide angle region are observed in the X-ray pattern of 8O-PD at 190°C as shown in Figure 4(b). The X-ray pattern of 8O-PD would be similar to that of a smectic phase. The d-spacing between smectic layers based on the peak in the small angle region is 31.5 Å. The calculated molecular length of 8O-PD with extended methylene conformation is 43 Å. Therefore we consider that director of 8O-PD should be tilted in the layer (smectic C phase, tilt angle: 43°), based upon the X-ray pattern and the observation of a schlieren texture or a thread texture. However, the phase transition entropy changes from mesophase to an isotropic liquid (ΔS_{MI}) for 8O-PD is 3.1 $\mathrm{Jmol^{-1}K^{-1}}$

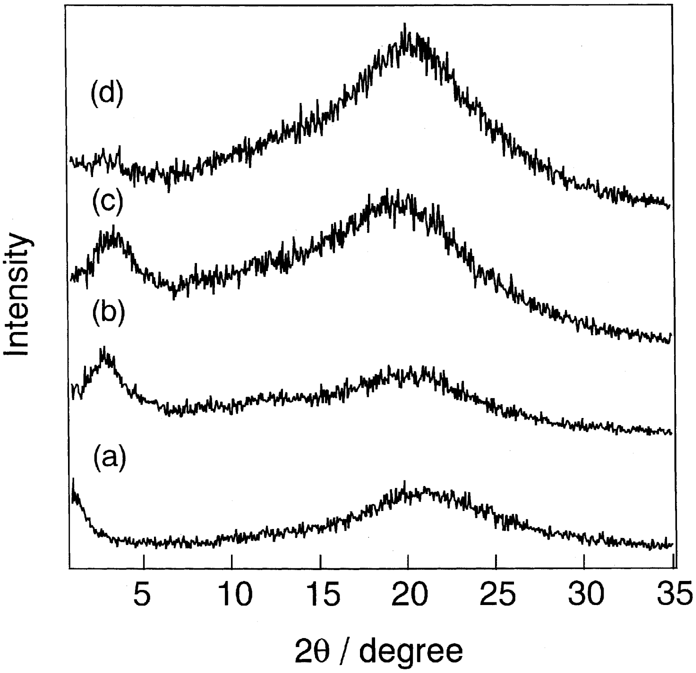

FIGURE 4 X-ray patterns of phosphorus derivatives in the mesomorphic temperature range; (a) 6O-PD at 200°C, (b) 8O-PD at 190°C, (c) 2MB-PD at 190°C, and (d) 2EO-PD at 150°C.

as shown in Table 1. The value of ΔS_{MI} for 8O-PD is smaller than that for 6O-PD, which is displaying a typical nematic phase. If 8O-PD exhibited a smectic C phase, the value of ΔS_{MI} for 8O-PD would be about 10 times larger than that of conventional nematic phase based on the higher orientational order of the mesogenic group in the smectic C phase [8]. Therefore, the structure of the mesophase for 8O-PD would be a cybotactic nematic phase due to the observation of a schlieren texture or a thread texture and the X-ray pattern similar to the smectic phase. The cybotactic nematic phase has the molecular array with smectic C order (cybotactic group) in nematic molecular array. The cybotactic group in the nematic structure is a cluster of LC molecules that form the molecular array similar to the smectic C phase. Both of the conventional nematic array of LC molecules and the cybotactic groups coexist in the cybotactic nematic phase [9–12].

Figure 4(c) shows the X-ray pattern of 2MB-PD at 190°C. The X-ray pattern of 2MB-PD is similar to that of 8O-PD. The d-spacing based on the peak in the small angle region of X-ray pattern for 2MB-PD is 24 Å. The calculated length of 2MB-PD with all-trans conformation is 35.6 Å. The d-spacing value of 2MB-PD and observation of the focal conic texture of 2MB-PD would allow us to estimate that the structure of the mesophase is an intercalated smectic structure proposed by Diele et al. [13,16], Weissflog and Demus [14], and Weissflog et al. On the other hand, Platé et al. reported that small peaks were observed in the small angle region of the X-ray pattern in the cholesteric phase [17]. In the possible model of the cholesteric phase, mesogenic groups are arranged in layers helically twisted along the axis normal to mesogenic groups. The structure of the mesophase of 2MB-PD could be similar to that of the cholesteric phase proposed by Platé et al. However, at the present time, we cannot exactly determine the structure of the mesophase of 2MB-PD.

Figure 4(d) displays the X-ray pattern of 2EO-PD where a broad peak in the wide angle region is observed. Temperature dependence of the X-ray pattern of 2EO-PD is not remarkable. The mesophase of 2EO-PD is assigned to a nematic phase based upon the observation of a schlieren texture as shown in Figure 1(d) and the X-ray diffraction pattern. The value of ΔS_{MI} of 2EO-PD is smaller than that of 6O-PD. Mesomorphic temperature range of 2EO-PD is wider than that of the phosphorus derivatives with alkoxy group. Furthermore, the nematic phase of 2EO-PD is fixed at room temperature.

Thermal degradation temperature (T_d) was recorded as a temperature at which 10% weight loss of the phosphorus derivatives occurs. Thermal degradation temperatures are summarized in Table 1. Some phosphorus derivatives are thermally stable until more than 300°C. Thermal decomposition temperature of 8O-PD is lower than that of other phosphorus

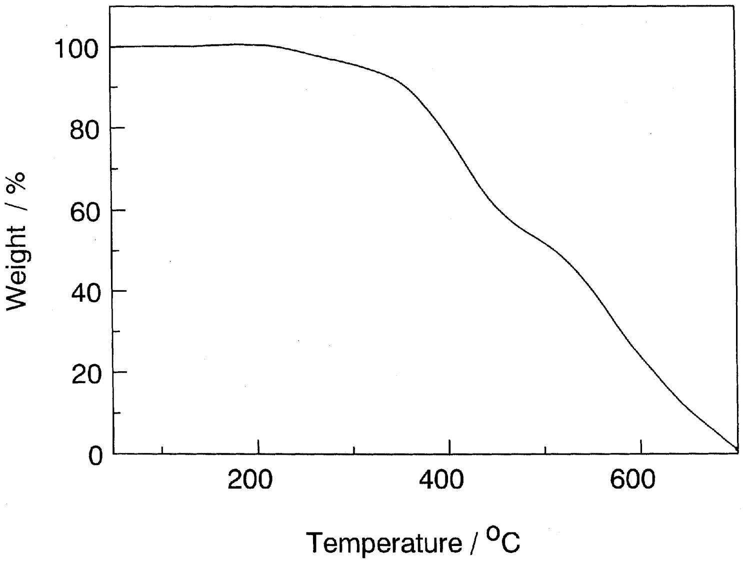

FIGURE 5 TGA curve of phosphorus derivatives (2MB-PD) in air.

derivatives, which have methylene chains as a terminal group of rigid moiety. At the present time, we cannot explain the phenomenon concerning the thermal decomposition of 8O-PD. Figure 5 shows a typical TGA curve of the phosphorus derivatives. Two main thermal degradation steps are observed in the TGA curve. The first step is detected in 350–450°C region, the other shows in the 500–650°C region. The details of the thermal degradation behavior are not clarified; however, the second step may be attributed to the partial degradation of phosphorus moiety [1].

REFERENCES

[1] Wang, C. S. & Lin, C. H. (1999). *Polymer*, *40*, 747–757.
[2] Annakutty, K. S. & Kishore, K. (1988). *Polymer*, *29*, 756–761.
[3] Kishore, K., Annakutty, K. S., & Mallick, I. M. (1988). *Polymer*, *29*, 762–764.
[4] Annakutty, K. S. & Kishore, K. (1988). *Polymer*, *29*, 1273–1276.
[5] Kannan, P., Gangadhara, & Kishore, K. (1991). *Polymer*, *32*, 1909–1913.
[6] Senthil, S. & Kannan, P. (2001). *J. Polym. Sci.: Part A: Polym. Chem.*, *39*, 2396–2403.
[7] Senthil, S. & Kannan, P. *J. Polym. Sci.: Part A: Polym. Chem.*, *40*, 2256–2263.
[8] Kumar, S. Ed., *Liquid Crystals: Experimental Study of Physical Properties and Phase Transitions*. Cambridge University Press: New York, (2001) p. 61.
[9] Kelker, H. & Hatz, R. Ed., *Handbook of Liquid Crystals*. Verlag Chemie: Weiheim, Deerfield Beach, FL, Basel, (1980) pp. 5, 26.
[10] de Vries, A. (1970). *Mol. Cryst. Liq. Cryst.*, *10*, 219–236.

[11] Blumstein, A., Vilasagar, S., Ponrathnam, S., Clough, S. B., & Blumstein, R. B. (1982). *J. Polym. Sci.: Polymer Physics Edition*, *20*, 877–892.

[12] Azároff, L. V. & Schuman, C. A. (1985). *Mol. Cryst. Liq. Cryst.*, *122*, 309–319.

[13] Diele, S., Weissflog, W., Pelzl, G., Manke, H., & Demus, D. (1986). *Liq. Crystals*, *1*, 101–105.

[14] Weissflog, W. & Demus, D. (1988). *Liq. Crystals*, *3*, 275–248.

[15] Weissflog, W., Demus, D., & Diele, S. (1990). *Mol. Cryst. Liq. Cryst.*, *191*, 9–15.

[16] Diele, S., Mädicke, A., Knauft, K., Neutzler, J., Weissflog, W., & Demus, D. (1991). *Liq. Crystals*, *10*, 47–61.

[17] Platé, N. A., Talrose, R. V., Freidzon, Ya. S., & Shibaev, V. P., (1987). *Polymer J.*, *19*, 135–145.